General Solution Of Multifrequency Acousto-Optic Diffraction In Bragg Cells

Jieping Xu, Ningsheng Ma, David N. Sitter, William T. Rhodes

Jieping Xu, Ningsheng Ma, David N. Sitter, William T. Rhodes, "General Solution Of Multifrequency Acousto-Optic Diffraction In Bragg Cells," Proc. SPIE 0936, Advances in Optical Information Processing III, (22 August 1988); doi: 10.1117/12.946927

SPIE.

Event: 1988 Technical Symposium on Optics, Electro-Optics, and Sensors, 1988, Orlando, FL, United States

General Solution of Multifrequency Acousto-Optic Diffraction in Bragg Cells

Jieping Xu

Georgia Institute of Technology, School of Electrical Engineering, Atlanta, Georgia 30332
On leave from Beijing Polytechnic University, Department of Applied Physics, Beijing, China

Ningsheng Ma

Tongji University, Department of Physics, Shanghai, China

David N. Sitter and William T. Rhodes

Georgia Institute of Technology, School of Electrical Engineering, Atlanta, Georgia 30332

Abstract

A general method for calculating the scattering amplitude of multifrequency acousto-optic diffraction is established. The method is based on counting allowable Feynman diagrams. It is found that the ratio of the number of Feynman diagrams allowable in the Bragg regime (isotropic, birefringent, and degenerate) to that in the Raman-Nath regime is independent of the total number of different acoustic frequencies, being a function only of the order of the Feynman diagram and the diffraction order of the final state. A general expression for this ratio is obtained. With this as a basis, complete perturbation solutions of the scattering amplitude can be obtained for any final state, any number of acoustic frequencies, and any kind of multifrequency acousto-optic diffraction. The theory is verified by comparing with theoretical results obtained previously and with experiment results.

1. Introduction

The theory of multifrequency acousto-optic (AO) diffraction is very important both in practical applications and in theory. Many sophisticated applications of AO devices are based on multifrequency AO diffraction, including the multi-channel AO modulators used in laser printers[1], AO spectrum analyzers[2], and AO devices used for interconnections in optical computing[3]. The theory of multifrequency AO diffraction has been incomplete, since the complete solution for the scattering amplitude in multifrequency AO diffraction has never been obtained for the Bragg regime (including the case of degenerate birefringent Bragg diffraction). That situation is remedied in this paper.

The theory of multifrequency acousto-optic (AO) diffraction was first investigated by Hecht[4], who derived an analytical solution to the coupled-mode equations in the Raman-Nath regime. For the Bragg regime case, Hecht obtained a perturbation solution (i.e., a power series solution) for the case of $N = 2$, N denoting the total number of different acoustic frequencies present. For cases of $N > 2$, only the leading term in the perturbation solution was obtained, and that only for some important final states (i.e., outgoing light beams). However, working only with the leading term is usually insufficient when the phase shift induced by the AO effect is not small. Korpel and Poon pointed out that the diffraction efficiency for both Raman-Nath and Bragg diffraction can be obtained through an approach based on Feynman diagrams, and considered the single-frequency ($N = 1$) case[5]. Recently, I. C. Chang pointed out that the Feynman-diagram method is universal and can be used to obtain the nonlinear responses due to both multifrequency AO diffraction and nonlinear acoustics[6]. In his paper he obtains the leading term in the perturbation solution for the case of two-tone and third order intermodulation.

In this paper, a complete solution for multifrequency AO diffraction with any N value is obtained

through the Feynman diagram approach. The diffraction can be Raman-Nath (R-N), Bragg (B), axial birefringent Bragg (AB), or rediffractable birefringent Bragg (RB). The foundation of this approach is based on counting the number of allowable Feynman diagrams (or allowable paths). In the following these are denoted by M^{R-N}, M^{B}, M^{AB}, and M^{RB}, respectively.

The following three important assertions about the ratios q of M^{B}, M^{AB}, and M^{RB} to M^{R-N} have been established through numerous drawings and calculations as will be explained below: (1) The ratios q are independent of the value of N, and thus a general expression for q can be obtained through consideration of the simplest case N = 1. (2) The dependence of q on the path cluster (a term defined below) is only through the order P of the path. (3) The dependence of q on the final state is only through the value of the diffraction order G. That is, all ratios q are functions of P and G only, not of N. Since all possible paths in any path cluster are allowable in the Raman-Nath regime, M^{R-N} can always be obtained using the knowledge of combinations and permutations. Thus, a complete solution can be obtained for any kind of multifrequency AO diffraction. In this paper, solutions for some typical final states will be given: the complete solution will be published elsewhere[7]. The theoretical results are verified by comparing with the experimental results.

2. Theory

2.1 Analysis of Final States

In single-frequency AO diffraction the outgoing light beams (hereafter referred to as the final states) can be denoted by a single integer, the diffraction order m; for multifrequency AO diffraction the final states must be denoted by a string of N integers $(m_1, m_2, \cdots, m_N) \equiv (m)$, where N is the total number of different frequencies involved in the interaction. Any final state can be represented by points with integer coordinates in a N-dimensional space, the state space. The frequency shift of final state (m) is given by

$$f = \sum_{i=1}^{N} m_i f_i \ . \tag{1}$$

Consistent with Ref. [4], the diffraction order G and the interaction order D of the final state (m) are defined by

$$G \equiv \sum_{i=1}^{N} m_i \ , \tag{2}$$

$$D \equiv \sum_{i=1}^{N} |m_i| \ . \tag{3}$$

As is well known, the leading term in the scattering amplitude of the final state with D is of the order of $(v/2)^D$, where v is the phase shift induced by the AO effect.

All the independent final states with $D \le 5$ are shown in Fig. 1 for the case of N = 2. The curve of D = const. is a square with its center at the origin and its four vertices at coordinate axes. The curve of G = const. is a straight line making an angle of -45° to the coordinate axes. Final states on both sides of the straight lines G = 0 and $m_1 = m_2$ are equivalent. Thus, only final states within a quarter square need be considered. The situation is similar for other values of N. If the order of approximation desired is D_0, only final states with $D \le D_0$ should be considered. Final states with negative G values are equivalent to those with positive G values and only final states with $G \ge 0$ need be considered. Also, final states obtained by all permutations of the same string of integer numbers (m) are equivalent to each other. For example, the total number of the three-tone third order

intermodulation states $f_i + f_j - f_k$ is $P(N, 3) = N(N - 1)(N - 2)$; however, only one representative case--$f_1 + f_2 - f_3$, for example--need be considered.

2.2 Feynman diagram approach of multifrequency AO diffraction

2.2.1 General Idea. In Refs. [4] and [5], the function $E^G_{(m)}(z)$ is derived. We are interested in the value of this function after the AO interaction is finished. That is, only the so-called scattering amplitude

$$\Psi_G(f) \equiv E^G_{(m)}(L)$$

is useful. (Here the frequency shift f as defined by Eq. (1), instead of (m), is used to label the scattering amplitude in accordance with the custom in multifrequency AO diffraction.) Rather than calculate $E^G_{(m)}(z)$, it is much simpler to obtain the scattering amplitude $\Psi_G(f)$ using the Feynman diagram approach since in this case the Feynman path integral is only an integral over the energy-momentum. Moreover, if only the results for the case when the momentum match condition is fulfilled are needed (as will usually be the case), then the Feynman path integral can be carried out trivially. The only task is counting the number M of allowable Feynman diagrams. (It might be noted that the Feynman diagram was developed originally for obtaining the S-matrix, which gives the scattering amplitude between any pair of initial and final states before and after the scattering process.[8] The situations are thus quite similar.)

A second simplification in analyzing multifrequency AO diffraction lies in describing the elementary AO interactions by

$$\begin{aligned} \omega_d &= \omega_i \pm \Omega_i , \\ \mathbf{k}_d &= \mathbf{k}_i \pm \mathbf{K}_i . \end{aligned} \tag{4}$$

This says that only one phonon can be absorbed or released by the incident photon, a condition that is essential for the establishment of the coupled-wave equation. In this case, any Feynman diagram such as shown in Fig. 2 can be represented by a path in the N-dimensional state space such as shown in Fig. 3. The elementary AO interactions of Eq. (4) are represented by

$$\begin{aligned} &\text{step i:} \quad \hat{m}_i = \hat{m}_i + 1, \text{ and } \hat{m}_j = \hat{m}_j \text{ for all } j \neq i , \\ &\text{step } \bar{\text{i}}\text{:} \quad \hat{m}_i = \hat{m}_i - 1, \text{ and } \hat{m}_j = \hat{m}_j \text{ for all } j \neq i , \end{aligned} \tag{5}$$

where $\hat{m}_i$ ($i = 1, 2, \cdots, N$) is a set of N variables that change their values according to Eq. (5) during each step. Its initial value is the initial state (0) and its final value in the final state (m). Thus, a path is a continuous zigzag line, line segments parallel to the coordinate axes, between the origin (0) and the final state (m). The number of vertices in any Feynman diagram (or the number of steps in the corresponding path) is called the *order P* of the path (or Feynman diagram). As indicated by Eq. (7) below, the contribution of a P^{th}-order path to the scattering amplitude is of the order of $(v/2)^P$. It is easy to see that all possible values of P are

$$P = D, D + 2, D + 4, \cdots . \tag{6}$$

The upper limit of P is determined by the order of approximation desired. All paths that can be obtained by permutations of the same string of steps are said to form a *path cluster*. Figure 3 gives three examples of path clusters, all between the initial state (0) and the final state (1, 0, 0, ···, 0): path cluster {1} with P = 1 containing only one path; path cluster {1, 1, $\bar{1}$} with P = 3 containing C(3, 1) = 3 paths; and path cluster {1, 2, $\bar{2}$} with P = 3 containing 3! = 6 paths.

The contribution of each Feynman diagram (or each path) to the scattering amplitude is easy to obtain if the momentum match condition is fulfilled. Let us consider a Feynman diagram of order P which consists of r_i steps i and s_i steps $\bar{i}$ (i = 1, 2, ..., N). Of course, we must have

$$\sum_{i=1}^{N} (r_i + s_i) \equiv \sum_{i=1}^{N} p_i = P .$$

Now, step i is in fact a +1 order AO interaction with the signal f_i. Its contribution to the scattering amplitude is given by $v_i/2$, where v_i is the phase shift induced by the AO effect of the i^{th} signal. Likewise, the step $\bar{i}$ is a -1 order AO interaction with f_i, and its contribution is given by $-v_i/2$. By noting that the total number of permutations of P steps is P!, the contribution to the scattering amplitude corresponding to this Feynman diagram is easliy shown to be

$$\frac{1}{P!} \prod_{i=1}^{N} \left(\frac{v_i}{2} \right)^{r_i} \left(- \frac{v_i}{2} \right)^{s_i} = \frac{1}{P!} \prod_{i=1}^{N} (-1)^{s_i} \left(\frac{v_i}{2} \right)^{p_i} . \tag{7}$$

It should be emphasized that the value given by Eq. (7) depends only on numbers r_i and s_i of steps and is independent of the position where each definite step appears. Thus, all paths (all Feynman diagrams) that belong to the same path cluster will give the same contribution (7). Multiplying Eq. (7) by the number M of allowable paths in each path cluster yields the contribution of the whole path cluster. Adding contributions of all possible path clusters yields the desired scattering amplitude, that is,

$$\Psi_G(f) = \sum_{P} \Psi_G^{(P)}(f) = \sum_{P} \sum_{clu} M \frac{1}{P!} \prod_{i=1}^{N} (-1)^{s_i} \left(\frac{v_i}{2} \right)^{p_i} , \tag{8}$$

where the second summation is over all possible P^{th} order path clusters. Thus, in fact, we need not to know in detail what kinds of paths are contained in each path cluster; only the number M of allowable paths in each path cluster is important. As soon as the numbers M for all possible path clusters are determined, the scattering amplitude can easily be obtained by Eq. (8).

2.2.2 Methods of evaluating numbers M and important conclusions. For Raman-Nath diffraction, there is no restriction on the path shape. That is, at any step of a path, +1 order and -1 order elementary AO interactions [Eq. (4)] are always allowable. Thus, in the Raman-Nath regime, the number $M^{R\text{-}N}$ of allowable paths in any path cluster is just equal to the number of all possible paths in that path cluster and can easily be obtained by the knowledge of combinations and permutations. However, for Bragg diffraction (both isotropic and non-degenerate birefringent Bragg diffraction) and degenerate birefringent Bragg diffraction* (including axial degenerate birefringent and rediffractable degenerate birefringent Bragg diffraction as shown in Fig. 4), the restrictions

---

* *In the literature, the rediffractable diffraction named here is called the degenerate diffraction*[9]. However, since the axial and rediffractable diffraction are all working near the degenerate frequency f_d, it seems more reasonable to retain the name degenerate for both.

$$
\begin{aligned}
&0 \le \hat{G} \equiv \sum_{i=1}^{N} \hat{m}_i \le 1 \quad \text{(for B)}, \\
&-1 \le \hat{G} \le 1 \quad \text{(for AB)}, \\
&0 \le \hat{G} \le 2 \quad \text{(for RB)},
\end{aligned} \tag{9}
$$

due to momentum match condition must always be fulfilled at any step of a path[5]. Geometrically, an allowable path in the Bragg regime must lie entirely within the region bounded by two superplanes G = 0 and 1, G = -1 and 1, or G = 0 and 2. There are two methods to evaluate the number of allowable paths in the Bragg regime: geometrically and by computer. In the geometrical method, we simply draw out all possible paths in any path cluster and check by inspection which paths lie entirely within the region bounded by the two superplanes. This method is intuitive, easy to do for the cases N = 1 and 2, and possible for the case of N = 3. In the computer method, a computer program is designed that generates all possible paths in sequence and checks Eq. (9) at each step. If Eq. (9) is violated at any step of a path, this path will be rejected.

Through numerous drawings (the first method) and calculations (the second method), the three important assertions mentioned in Sect. 1 have been verified for all cases with P ≤ 10. We consider this sufficient to cover all practical purposes. Moreover, we consider it highly probable that these assertions are valid universally, even though a rigorous proof has not yet been found. Thus, we believe that all the ratios

$$
q^{B} \equiv \frac{M^{B}}{M^{R\text{-}N}}, \quad q^{AB} \equiv \frac{M^{AB}}{M^{R\text{-}N}}, \quad q^{RB} \equiv \frac{M^{RB}}{M^{R\text{-}N}}
$$

for any path cluster and any final states are independent of the value of N and are only dependent on the value of P and G.

2.2.3 General expressions of ratios q(P, G). Since the ratios q(P, G) are independent of the value of N, their general expressions can be obtained by considering the simplest case N = 1. The results are as follows:

$$
\begin{aligned}
&q^{B}(P, 0) = q^{B}(2t, 0) = \frac{1}{C(2t, t)} = \frac{t!\,t!}{2t!}, \\
&q^{B}(P, 1) = q^{B}(2t+1, 1) = \frac{1}{C(2t+1, t)} = \frac{t!\,(t+1)!}{(2t+1)!}; \\
&q^{AB}(P, 0) = q^{AB}(2t, 0) = \frac{2^{t}\,t!\,t!}{(2t)!}, \\
&q^{AB}(P, 1) = q^{AB}(2t+1, 1) = \frac{2^{t}\,t!\,(t+1)!}{(2t+1)!}; \\
&q^{RB}(P, 0) = q^{RB}(2t, 0) = \frac{2^{t-1}\,t!\,t!}{(2t)!}, \\
&q^{RB}(P, 1) = q^{RB}(2t+1, 1) = \frac{2^{t}\,t!\,(t+1)!}{(2t+1)!}, \\
&q^{RB}(P, 2) = q^{RB}(2t+2, 2) = \frac{2^{t}\,t!\,(t+2)!}{(2t+2)!}.
\end{aligned} \tag{10}
$$

The specific values of q(P, G) for P ≤ 10 can easily be calculated from Eq. (10) and are listed in Table 1. They have been verified for all possible cases by the computer method mentioned above and are probably sufficient for all cases of practical interest. For any path cluster, the number M in the Bragg regime can be obtained by multiplying the values of q(P, G) by the corresponding numbers $M^{R\text{-}N}$. The scattering amplitude can be obtained by using Eq. (8); the intensities of outgoing light beams are given by the squares of the corresponding scattering amplitudes.

Table 1. Specific values of q(P, G) with P ≤ 10

Values of q(P, 0)

P	0	2	4	6	8	10
Bragg (B)	1	1/2	1/6	1/20	1/70	1/252
Axial (AB)	1	1	2/3	2/5	8/35	8/63
Rediff. (RB)	1	1/2	1/3	1/5	4/35	4/63

Values of q(P, 1)

P	1	3	5	7	9
Bragg (B)	1	1/3	1/10	1/35	1/126
Axial (AB)	1	2/3	2/5	8/35	8/63
Rediff. (RB)	1	2/3	2/5	8/35	8/63

Values of q(P, 2)

P	0	2	4	6	8	10
Rediff. (RB)	1	1	1/2	4/15	1/7	8/105

3. Examples of Calculating Scattering Amplitudes and Intensities

3.1 Scattering amplitude in Raman-Nath regime

Let us first consider the case of N = 2. The final state can be expressed generally by (m_1, m_2). All possible path clusters are composed of $s + m_1$ steps 1, s steps $\bar{1}$, $t + m_2$ steps 2, and t steps $\bar{2}$ with $P = 2s + m_1 + 2t + m_2$ (s, t = 1, 2, ···). The numbers of allowable paths are given by

$$M^{R\text{-}N} = C(2s+m_1+2t+m_2, s)\cdot C(s+m_1+2t+m_2, t)\cdot C(s+m_1+t+m_2, t+m_2)$$
$$= \frac{(2s+m_1+2t+m_2)!}{s!\,(s+m_1)!\,t!\,(t+m_2)!} .$$

By Eq. (8), the scattering amplitudes are given by

$$\Psi_G(m_1f_1 + m_2f_2) = \sum_{s=0}^{\infty}\sum_{t=0}^{\infty} M^{R\text{-}N}\frac{(-1)^{s+t}}{(2s+m_1+2t+m_2)!}\left(\frac{v_1}{2}\right)^{2s+m_1}\left(\frac{v_2}{2}\right)^{2t+m_2}$$
$$= \sum_{s=0}^{\infty}\sum_{t=0}^{\infty}\frac{(-1)^{s+t}}{s!(s+m_1)!t!(t+m_2)!}\left(\frac{v_1}{2}\right)^{2s+m_1}\left(\frac{v_2}{2}\right)^{2t+m_2}$$
$$= J_{m_1}(v_1)\cdot J_{m_2}(v_2) ,$$

where the power series expansion of the Bessel function[10]

$$J_m(v) = \sum_{t=0}^{\infty} \frac{(-1)^t}{t!\,(t+m)!} \left(\frac{v}{2}\right)^{2t+m}$$

is used. Obviously, such a procedure can also be used for the case of any N value, and the scattering amplitude is given by

$$\Psi_G(f) = \prod_{i=1}^{N} J_{m_i}(v_i) \,. \tag{11}$$

Equation (11) is exactly the same as those obtained from the coupled-wave equation[4], but the derivation is much simpler here.

3.2 Scattering amplitude of three-tone third order intermodulation state

As mentioned above, only a representative $f_1 + f_2 - f_3$ needs to be considered. The final state is (1, 1, -1, 0, 0, ···, 0) with G = 1 and D = 3. We calculate this scattering amplitude up to P = 5. All possible path clusters as well as their corresponding values of $M^{R\text{-}N}$, $q^B(P, 1)$ from Table 1, and $M^B = q^B(P, 1)M^{R\text{-}N}$ are all listed in Table 2.

Table 2 All possible path clusters for the intermodulation state $f_1 + f_2 - f_3$ and their $M^{R\text{-}N}$, $q^B(P, 1)$, and M^B values.

P	path cluster	$M^{R\text{-}N}$	$q^B(P, 1)$	M^B
3	$\{1, 2, \bar{3}\}$	3! = 6	1/3	2
5	$\{1, 1, \bar{1}, 2, \bar{3}\}$	C(5, 2)·3! = 60	1/10	6
	$\{1, 2, 2, \bar{2}, \bar{3}\}$	C(5, 2)·3! = 60	1/10	6
	$\{1, 2, 3, \bar{3}, \bar{3}\}$	C(5, 2)·3! = 60	1/10	6
	$\{1, 2, \bar{3}, i, \bar{i}\}$ $(i \neq 1, 2, 3)$	5! = 120	1/10	12

By Eq. (8), it is easy to obtain the scattering amplitude as

$$\Psi_1(f_1 + f_2 - f_3) \simeq \Psi_1^{(3)}(f_1 + f_2 - f_3) + \Psi_1^{(5)}(f_1 + f_2 - f_3) \,,$$

$$\Psi_1^{(3)}(f_1 + f_2 - f_3) = -\frac{1}{3}\left(\frac{v_1}{2}\right)\left(\frac{v_2}{2}\right)\left(\frac{v_3}{2}\right) \,,$$

$$\Psi_1^{(5)}(f_1 + f_2 - f_3) = \frac{1}{20}\left(\frac{v_1}{2}\right)^3\left(\frac{v_2}{2}\right)\left(\frac{v_3}{2}\right) \tag{12}$$

$$+ \frac{1}{20}\left(\frac{v_1}{2}\right)\left(\frac{v_2}{2}\right)^3\left(\frac{v_3}{2}\right) + \frac{1}{20}\left(\frac{v_1}{2}\right)\left(\frac{v_2}{2}\right)\left(\frac{v_3}{2}\right)^3$$

$$+ \frac{1}{10}\left(\frac{v_1}{2}\right)\left(\frac{v_2}{2}\right)\left(\frac{v_3}{2}\right)\sum_{i=4}^{N}\left(\frac{v_i}{2}\right)^2 \,,$$

where the label "B" is omitted for simplicity. Specifically, if all v_i are equal, Eq. (12) simplifies to

$$\Psi_1(f_i + f_j - f_k) \simeq \Psi_1^{(3)}(f_i + f_j - f_k) + \Psi_1^{(5)}(f_i + f_j - f_k) ,$$

$$\Psi_1^{(3)}(f_i + f_j - f_k) = -\frac{1}{3}\left(\frac{v}{2}\right)^3 , \tag{13}$$

$$\Psi_1^{(5)}(f_i + f_j - f_k) = \frac{2N-3}{20}\left(\frac{v}{2}\right)^5 .$$

Since all three-tone third-order intermodulation cases result in the same scattering amplitude when all v_i are equal, the label is changed to the general form $f_i + f_j - f_k$. The scattering amplitude of the degenerate birefringent Bragg diffraction can be obtained directly from the result of the Bragg diffraction. In fact, we have

$$\Psi_G^{(P)}(f, AB) = \frac{q^{AB}(P, G)}{q^{B}(P, G)} \Psi_G^{(P)}(f, B).$$

3.3 Scattering amplitude and intensity of zero order state

As a final example, we calculate the scattering amplitude and intensity of the zero order state, i.e., the state (0) with G = D = 0. Of necessity, the perturbation solution of $\Psi_0(0)$ contains the greatest number of terms. The value of $\Psi_0(0)$ is most sensitive to the value of N and its computational convergence is thus slowest, since all diffracted beams (principal and intermodulated) eventually come from the zero-order beam. We shall calculate this perturbation solution up to P = 6. All possible path cluster as well as their corresponding values of $M^{R\text{-}N}$, $q^B(P, 0)$ from Table 1, and M^B are listed in Table 3. In the table, { } denotes an empty path cluster, its path containing no step (no AO interaction) at all.

Table 3 All possible path cluster for the zero order state f = 0 and their $M^{R\text{-}N}$, $q^B(P, 0)$, and M^B values.

P	path cluster	$M^{R\text{-}N}$	$q^B(P, 1)$	M^B
0	{ }	C(0, 0) = 1	1	1
2	{i, $\bar{i}$}	2! = 2	1/2	1
4	{i, i, $\bar{i}$, $\bar{i}$}	C(4, 2) = 6	1/6	1
	{i, $\bar{i}$, j, $\bar{j}$} (j ≠ i)	4! = 24	1/6	4
6	{i, i, i, $\bar{i}$, $\bar{i}$, $\bar{i}$}	C(6, 3) = 20	1/20	1
	{i, i, $\bar{i}$, $\bar{i}$, j, $\bar{j}$} (j ≠ i)	C(6, 2)·C(4, 2)·2! = 180	1/20	9
	{i, $\bar{i}$, j, j, $\bar{j}$, $\bar{j}$} (j ≠ i)	C(6, 2)·C(4, 2)·2! = 180	1/20	9
	{i, $\bar{i}$, j, $\bar{j}$, k, $\bar{k}$} (k ≠ j ≠ i)	6! = 720	1/20	36

By Eq. (8), the scattering amplitude is given by

$$\Psi_0(0) \simeq \Psi_0^{(0)}(0) + \Psi_0^{(2)}(0) + \Psi_0^{(4)}(0) + \Psi_0^{(6)}(0) ,$$

$$\Psi_0^{(0)}(0) = 1 ,$$

$$\Psi_0^{(2)}(0) = -\frac{1}{2}\sum_{i=1}^{N}\left(\frac{v_i}{2}\right)^2 ,$$

$$\Psi_0^{(4)}(0) = \frac{1}{24}\sum_{i=1}^{N}\left(\frac{v_i}{2}\right)^4 + \frac{1}{6}\sum_{i=1}^{N}\sum_{j=i+1}^{N}\left(\frac{v_i}{2}\right)^2\left(\frac{v_j}{2}\right)^2 \qquad (14)$$

$$\Psi_0^{(6)}(0) = -\frac{1}{720}\sum_{i=1}^{N}\left(\frac{v_i}{2}\right)^6$$
$$-\frac{1}{80}\sum_{i=1}^{N}\sum_{j=i+1}^{N}\left(\frac{v_i}{2}\right)^4\left(\frac{v_j}{2}\right)^2 - \frac{1}{80}\sum_{i=1}^{N}\sum_{j=i+1}^{N}\left(\frac{v_i}{2}\right)^2\left(\frac{v_j}{2}\right)^4$$
$$-\frac{1}{20}\sum_{i=1}^{N}\sum_{j=i+1}^{N}\sum_{k=j+1}^{N}\left(\frac{v_i}{2}\right)^2\left(\frac{v_j}{2}\right)^2\left(\frac{v_k}{2}\right)^2 .$$

Specifically, if all v_i are equal, Eq. (14) simplifies to

$$\Psi_0(0) \simeq \Psi_0^{(0)}(0) + \Psi_0^{(2)}(0) + \Psi_0^{(4)}(0) + \Psi_0^{(6)}(0) ,$$

$$\Psi_0^{(0)}(0) = 1 ,$$

$$\Psi_0^{(2)}(0) = -\frac{N}{2}\left(\frac{v}{2}\right)^2 , \qquad (15)$$

$$\Psi_0^{(4)}(0) = \frac{2N^2 - N}{24}\left(\frac{v}{2}\right)^4 ,$$

$$\Psi_0^{(6)}(0) = -\frac{6N^3 - 9N^2 + 4N}{720}\left(\frac{v}{2}\right)^6 .$$

In obtaining the last equation, the identity $1\cdot2 + 2\cdot3 + \cdots + (N-2)(N-1) = N(N-1)(N-2)/3$ (verified by the method of induction) is used. The intensity of the zero order beam is given by $|\Psi_0(0)|^2$. We shall only write down here its expression when all v_i are equal. By Eq. (15), we get

$$I_0(0) \simeq I_0^{(0)}(0) + I_0^{(2)} + I_0^{(4)}(0) + I_0^{(6)}(0) ,$$

$$I_0^{(0)}(0) = |\Psi_0^{(0)}(0)|^2 = 1 ,$$

$$I_0^{(2)}(0) = 2\Psi_0^{(0)}(0)\Psi_0^{(2)}(0) = -N\left(\frac{v}{2}\right)^2 ,$$

(16)

$$I_0^{(4)}(0) = |\Psi_0^{(2)}(0)|^2 + 2\Psi_0^{(0)}(0)\Psi_0^{(4)}(0)$$
$$= \frac{5N^2 - N}{12}\left(\frac{v}{2}\right)^4 ,$$

$$I_0^{(6)}(0) = 2\Psi_0^{(2)}(0)\Psi_0^{(4)}(0) + 2\Psi_0^{(0)}(0)\Psi_0^{(6)}(0)$$
$$= -\frac{9N^3 - 6N^2 + N}{90}\left(\frac{v}{2}\right)^6 .$$

A general expression (up to the sixth order of approximation but for any N value) for the depletion $d \equiv 1 - I_0(0)$ can immediately be obtained. It has been found that the perturbation solution for intensities converges much slower than that for scattering amplitude. Thus, if only numerical values (instead of general expressions) for intensities are needed, it is suggested to calculate them through the square of the numerical values of the corresponding scattering amplitude.

Although only three examples are considered here, it is obvious that scattering amplitudes and intensities of any final state and for any N value can be obtained up to any order of approximation desired by the Feynman diagram approach.

4. Experimental Verification of the Theory

For the verification of the theory, we shall mainly consider the case of N = 2 since the total number of intermodulation states increases rapidly and to measure them separately becomes rather difficult. Because we have not written down solutions for all final states in this paper, only results are given even for the theoretical value.

4.1 Verification of the theory for the Bragg diffraction

As pointed out in Reference [4], for the case of N = 2 and $v_1 = v_2 = v$, an analytical (or rigorous) solution can be obtained for the scattering amplitude and is given by

$$\Psi_0(0) = J_0(v) , \quad \Psi_1(f_i) = J_1(v) ,$$
$$\Psi_0(f_i - f_j) = J_2(v) , \quad \Psi_1(2f_i - f_j) = J_3(v) , \qquad (17)$$
$$\Psi_0(2f_i - 2f_j) = J_4(v) , \quad \Psi_1(3f_i - 2f_j) = J_5(v).$$

On the other hand, for N = 2, Eq. (15) simplifies to

$$\Psi_0(0) \simeq 1 - \left(\frac{v}{2}\right)^2 + \frac{1}{4}\left(\frac{v}{2}\right)^4 - \frac{1}{36}\left(\frac{v}{2}\right)^6 .$$

For v/2 = 0.8, the successive values of $\Psi_0(0)$ calculated from the above equation when more terms are considered is 1, 0.36, 0.4624, and 0.4551; while the rigorous value is $J_0(1.6) = 0.4554$. Thus, even for the case of N = 2, the contribution of higher order terms may be important. It is easy to see from Eq. (15) that the contribution of higher order terms will be more important for larger N values. A more complete comparison of values of our perturbation solution when different orders of approximation are considered with the rigorous theoretical value and with the measured value are summarized in Table 3.

The AO deflector used was a glass device with planar phase array manufactured by IntraAction Corp.

Table 3 Comparison of values of our perturbation solution (up to different orders of approximation considered) with the rigorous theoretical values and with the measured value. (v/2 = 0.8)

Final state	Order of approximation 0	2	4	6	Rigorous value	Measured value
$\|\Psi_0(0)\|^2$	100%	12.96%	21.38%	20.71%	20.74%	21%
$\|\Psi_0(f_i-f_j)\|^2$	-	10.24%	6.34%	6.61%	6.60%	2.7%
$\|\Psi_0(2f_i-2f_j)\|^2$	-	-	0.0291%	0.0222%	0.0226%	-

Final state	Order of approximation 1	3	5	Rigorous value	Measured value
$\|\Psi_1(f_j)\|^2$	64.00%	29.59%	32.64%	32.48%	34%
$\|\Psi_1(2f_i-f_j)\|^2$	-	0.728%	0.514%	0.526%	0.49%
$\|\Psi_1(3f_i-2f_j)\|^2$	-	-	0.00075%	0.00071%	-

4.2 Verification of the Theory for the Degenerate Birefringent Bragg Diffraction Case

The AO device used is a deviated but on-axis TeO_2 device designed for a compact Triple-Product-Processor system[11]. Originally, this device is designed for $\lambda_0 = 0.8$ μm with $f_0 = f_d = 92$ MHz. When used at $\lambda_0 = 0.6328$ μm, the measured degenerate frequency is $f_d = 116$ MHz. The length of the transducer is 3 mm, which corresponds to Q = 188. For the case of N = 1, the theoretical value of axial and rediffractable birefringent Bragg diffraction as well as the measured value for v/2 = 0.5 and 0.8 are summarized in Table 4. Also, for the case of N = 2, the theoretical and measured values for v/2 = 0.5 are summarized in Table 5. All the theoretical values in Tables 4 and 5 are up to the order of P = 5. The consistency between theory and experiment is good.

Table 4 Comparison of the theoretical and measured values of the axial and rediffractable birefringent Bragg diffraction for the case of N = 1. (v/2 = 0.5 and 0.8)

v/2 = 0.5	Axial Theoretical	Measured	Rediffractable Theoretical	Measured
$\|\Psi_0(0)\|^2$	57.8%	57.65%	77.8%	78.8%
$\|\Psi_0(f)\|^2$	21.1%	21.1%	21.1%	20.0%
$\|\Psi_2(2f)\|^2$	-	-	1.44%	1.66%

v/2 = 0.8	Axial Theoretical	Measured	Rediffractable Theoretical	Measured
$\|\Psi_0(0)\|^2$	18.34%	18.34%	51.0%	50.8%
$\|\Psi_0(f)\|^2$	41.0%	40.2%	41.0%	41.14%
$\|\Psi_2(2f)\|^2$	-	-	8.17%	11.4%

Table 5 Comparison of the theoretical and measured values of the axial and rediffractable birefringent Bragg diffraction for the case of N = 2. (v/2 = 0.5)

	Axial Theoretical	Measured	Rediffractable Theoretical	Measured
$\|\Psi_0(0)\|^2$	31.64%	31.64%	61.0%	60.3%
$\|\Psi_0(f_i-f_j)\|^2$	4.34%	5.67%	1.085%	1.033%
$\|\Psi_1(f_j)\|^2$	14.85%	14.67%	14.85%	14.85%
$\|\Psi_1(2f_i-f_j)\|^2$	0.1485%	0.18%	0.133%	0.127%

5. CONCLUSION

Through numerous drawings and calculations, the important conclusion has been established that the ratios q are independent of the value of N and are functions of P and G alone. Also, general expressions for these ratios q have been found. Then the scattering amplitude of any kinds of AO diffraction can easily be obtained for any final state and any N value through the Feynman diagram approach. The consistency between theory and experiment is good. Thus, the problem of multifrequency AO diffraction can be considered as completely solved. The method can be applied to obtain the response due to acoustical nonlinearities. Until now, only the two-tone and third-order intermodulation case has been considered, and only the leading term has been obtained.[12] The only difference is that the initial state becomes (1, 0, 0, ···, 0) instead of (0).

6. ACKNOWLEDGMENTS

This work was partially supported by the Joint Service Electronics Program under contract number DAAL03-87-K-0059.

7. REFERENCES

1. G. Hrbek and W. Watson, *Proc. of the Technical Program, EOSD Conference*, pp.271-xxx (1971 East).
2. D. L. Hecht, "Spectrum analysis using acousto-optic devices," *Proc. SPIE*, 90, pp. 148-157 (1976).
3. Special Issue on Optical Computing, *Proc. IEEE*, 72(7), pp. 758-974 (1984).
4. D. L. Hecht, "Multifrequency acoustoptic diffraction," *IEEE Trans. on Sonics and Ultrasonics*, SU-24(1), 7-18 (1977).
5. A. Korpel, "Two-dimensional plane wave theory of strong acousto-optic interaction in isotropic media," *J. Opt. Soc. Am.*, 69(5), 678-683 (1979); A. Korpel and T. C. Poon, "Explicit formalism for acousto-optic multiple plane-wave scattering," *J. Opt. Soc. Am.*, 70(7), 817-820 (1980); T. C. Poon and A. Korpel, "Feynman diagram approach to acousto-optic scattering in the near-Bragg region," *J. Opt. Soc. Am.*, 71(10), 1202-1208 (1981).
6. I. C. Chang, "Multifrequency acousto-optic interaction in Bragg cells," *Proc. SPIE*, 753, 97-102 (1987).
7. Jieping Xu et al, to be published.
8. A. Messiah, *Quantum Mechanics II*, p. 724-728, North-Holland (1962); R. J. Eden, P. V. Landshoff, D. I. Olive, and J. C. Polkinghorne, *The Analytic S-Matrix*, Ch. 1, Cambridge (1966).
9. A. W. Warner, D. L. White, and W. A.Bonner, "Acousto-optic light deflectors using optical activitity in paratellurite," *J. Appl. Phys.*, 43(11), 4489-4495 (1972).
10 W. H. Beyer, *Standard Mathematical Tables*, 27th ed., p. 349, CRC Press (1984).
11. Jieping Xu, E. D. Young, D. N. Sitter, and W. T. Rhodes, "New designs and measurements of TeO_2 Bragg cells used in compact triple-product-processor systems," this issue.
12. I. C. Chang and R. T. Weverka, "Multifrequency acousto-optic diffraction in wideband Bragg cells," *1983 IEEE Ultrasonics Symposium*, pp. 445-448; G. Elston and P. Kellman, "The effects of acoustic nonlinearities in acousto-optic signal processing systems," *1983 IEEE Ultrasonics Symposium*, pp. 449-453; M. L. Shah and P. S. Zerwekh, "Intermodulation in wideband Bragg cells," *1983 IEEE Ultrasonics Symposium*, pp.441-444; G. Elston, "Intermodulation products in acousto-optic signal processing systems," *1985 IEEE Ultrasonics Symposium*, pp. 391-397; D. R. Pape, "Acousto-optic Bragg cell intermodulation products," *1986 IEEE Ultrasonics Symposium*, pp. 387-391.

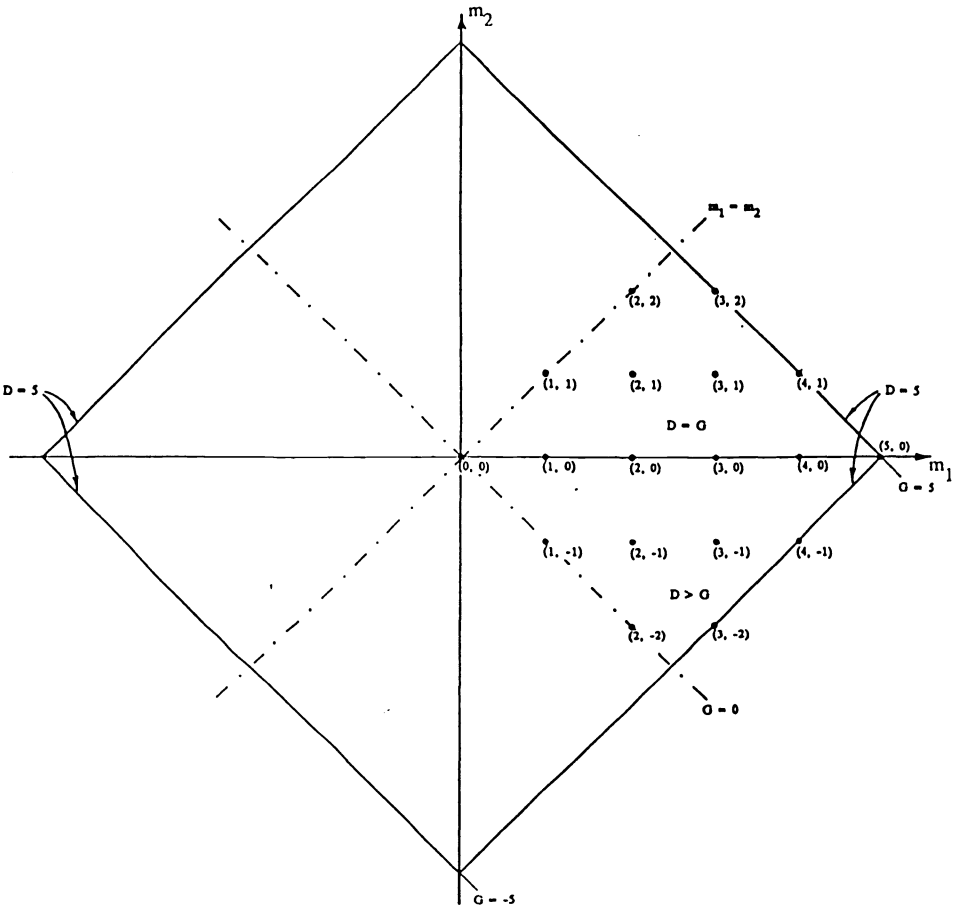

Fig. 1 The structure of final states (N = 2).

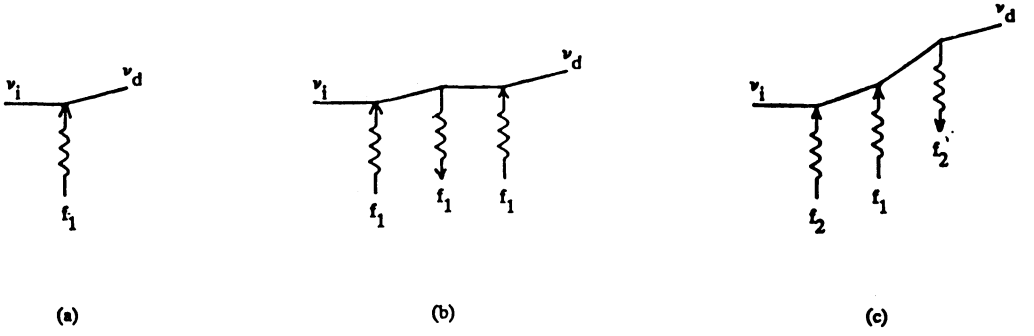

Fig. 2 Examples of the two lowest order (P = 1 and 3) Feynman diagrams corresponding to the final state (1, 0) or $\nu_d = \nu_i + f_1$.
(a) The first order P = 1;
(b) One possibility of the third order P = 3;
(c) Another possibility of the third order P = 3.

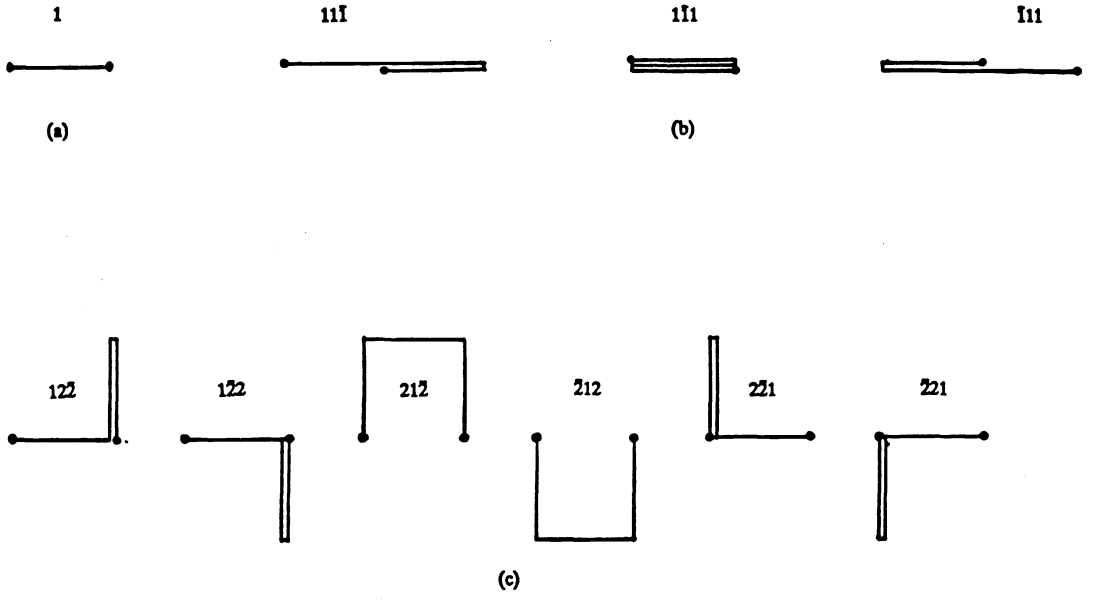

Fig. 3 The equivalent representation of Feynman diagrams by paths. All possible paths in the two lowest order (P = 1 and 3) path clusters for the case of N = 2 with the final state (1, 0).
(a) All possible paths in the path cluster {1};
(b) All possible paths in the path cluster {1, 1, 1̄};
(c) All possible paths in the path cluster {1, 2, 2̄}.

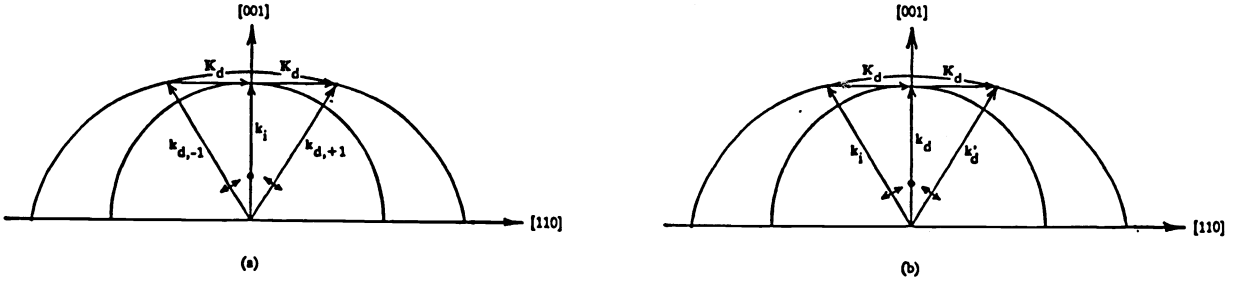

Fig. 4 The degenerated birefringent Bragg diffraction in the on-axis TeO_2 devices.
(a) The axial birefringent Bragg diffraction.
(b) The rediffractable birefringent Bragg diffraction.